An Analysis of Fireballs from Willamette's D6 AllSky Survey

by

Peter Joseph Gibson

Submitted in Partial Fulfillment of the
Requirements for the Degree

Bachelor of Arts

Supervised by
Dr. Jed Rembold

Department of Physics

Willamette University, College of Liberal Arts
Salem, Oregon

2019

Presentations and publications

P. Gibson, Analyzing Fireballs from Willamette's D6 AllSky Survey, Poster Presentation at Willamette University, Research Seminar II: Thesis Presentation (May 2019)

P. Gibson, Analyzing Fireballs from Willamette's D6 AllSky Survey, Oral Presentation at Willamette University, Research Seminar II: Thesis Presentation (April 2019)

P. Gibson, Analyzing Fireballs from Willamette's D6 AllSky Survey, Oral Presentation at Willamette University, Research Seminar I: Status Report Presentation (December 2018)

P. Gibson, Analyzing Fireballs from Willamette's D6 AllSky Survey, Oral Presentation at Willamette University, Advanced Techniques in Experimental Physics: Senior Proposal Presentation (April 2018)

Acknowledgments

I would like to thank the following professors for their tremendous support and advice throughout my Willamette experience:

- Dr. Jed Rembold for teasing me and providing me with Hershey's Kisses as a consolation for his hate.
- Dr. Rick Watkins for telling me "You got this!" in trying times.
- Dr. Daniel Borrero, Dr. Michaela Kleinart, Dr. David Altman for their kindness and unwavering confidence in our graduating class.

I would also so like to thank the following people for helping me through countless homework problems, talking down my problems, and also picking on me when I deserve it:

- Trent Jones for being a below par friend and an above par golfer.
- Jo Stensass for serving me all sorts of help along the way and providing a willingness to set me up for success.
- The wizards who answer questions on Stack Overflow and spend time editing Wikipedia to make it a more reliable resource.
- Not only to God but to Jesus

Lastly, but perhaps most importantly, I would like to thank my mother and father for their unconditional love and for providing me with countless wonderful life opportunities such as the entirety of my college experience. There is no argument that I would not be at this point without them.

Abstract

General Abstract

As fireballs, more commonly known as shooting stars, fly through Earth's atmosphere at breakneck speeds, they emit light that can be observed on our planet's surface. Willamette's D6 AllSky Survey is a camera system that probes the night's sky for these events which can be further utilized for large-scale analysis such as determining flux rates. Flux rates depict the number of events that occur per unit time per unit area. Because one camera system can only observe $< 0.4\%$ of Earth's total sky area, amateur astronomers hold a significant role in fireball observations. Their observations provide a robust data sample size that can then be used to gain a deeper understanding of the flux rates and property distributions of fireballs. While complex multi-camera professional systems currently exist, there is need for more economic, accessible, and versatile systems. We will discuss the feasibility of our current observational setup and how it compares to more elaborate existing systems.

Technical Abstract

Fireballs, more technically known as bolides, are recognizable by the light they emit through ablation. The D6 AllSky Camera was designed by Dr. Jed Rembold and Kyle McSwain as an alternative observation system for fireball research. It is smaller, more portable, and significantly cheaper than most existing systems used by professional astronomers. By measuring and comparing distributions of fireballs to other systems, primarily in the form of average flux, we aim to assess the feasibility of using the D6 AllSky Camera. Due to poor weather and other unforeseen complications, our data sample was not sufficiently large enough to produce a confident average flux rate. However the versatile framework established in this research will assuredly aid in the analysis of fireballs throughout further research.

Table of Contents

List of Figures

1 Introduction

Based on a rough estimate, there are about 10 000 trillion ants, 7.6 billion humans, and a few million elephants in the world. When considering this data set, one might come to the conclusion that there are more small objects in the world than there are large objects. It so happens that this conclusion not only holds true on Earth, but it also holds true in our universe. For every singular large object in space, there are significantly more smaller objects. To provide a parallel to the animal example, in our solar system, there is one star, eight planets, and an almost incomprehensible number of small rocks traveling through space.

In space, distances are presented on an extremely large scale when compared to on-Earth distances. Similarly objects in space travel significantly faster than objects observed on earth. For example, the Earth travels at approximately $30\,\mathrm{km\,s^{-1}}$ while small rocks can travel between $11\,\mathrm{km\,s^{-1}}$ to $70\,\mathrm{km\,s^{-1}}$. The speeds of these rocks exceed the muzzle velocity of a bullet [11]. When we observe a meteor shower, we are witnessing a barrage of these bullet-like rocks. Fortunately for mankind, Earth's atmosphere provides a protective shield. This shield is composed of tightly packed (relative to the vacuum of space) air molecules.

As a rocky object travels through Earth's atmosphere, it collides with particles and burns in a phenomena known as ablation. The result is a release of energy in the form of both heat and light. The objects, which ignite and begin to break down are called meteors. As a meteor releases light, the brightness can be measured from Earth's surface and is expressed as a photometric (visual) magnitude. The brightest meteors, which have a magnitude less than -4, are referred to as fireballs. By observing the magnitude, duration, and other properties of individual fireball events, an observer can estimate impact energies and sizes of these near-Earth rocky objects.

Studying these near-Earth objects can give us good estimates for how many objects you might expect to see pass through a given area of space within a specific amount of time. This measurement is called flux. By determining flux, we can more accurately predict the likelihood of objects in space being hit by near-Earth objects. Although the case may have been an extreme one, the space satellite

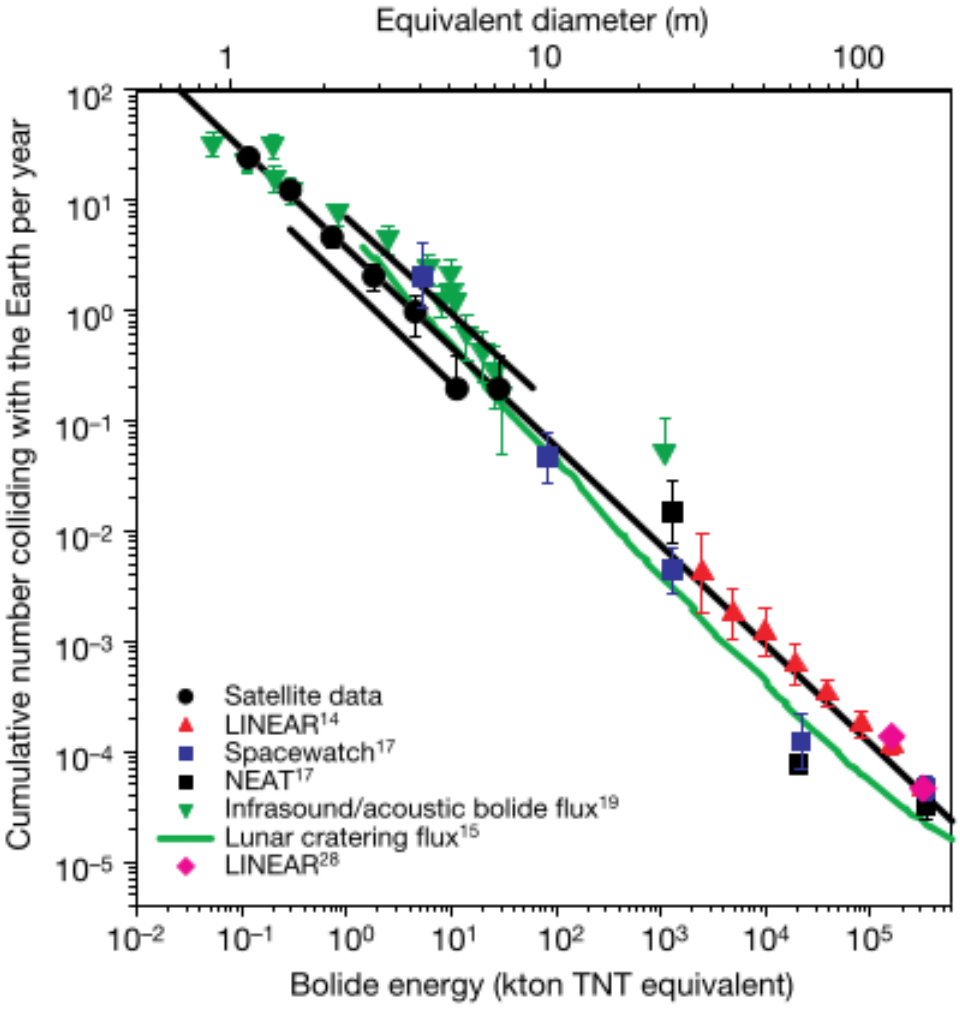

Figure 1.1: A plot of bolide flux vs. energy and diameter using a wide collection of data

Olympus was struck and destroyed by a meteoroid during the Perseid meteor shower in 1993 [1]. Additionally, given the relationships between the number of objects hitting earth per time for different objects, we can estimate the probability of extremely large impacts on earth. These estimates, similarly to predictions surrounding volcanic or earthquake activity, give us insight into past events and help us foresee likelihoods of future events.

This project aims to analyze the feasibility of the Willamette D6 AllSky camera, a new alternative camera system for conducting fireball research. Occupying about the same space as a traffic cone, this camera is easily transportable and does not require an expensive computational base. To determine the feasibility of our setup, we will compare our measured flux rates to those found by more well-

recognized systems. Peter Brown, an astronomy researcher, created a now-famous relationship between flux and bolide energy/diameter. As seen in Fig. 1.1, bolides with extremely high energies are far less likely to collide with earth than their less powerful counterparts. By comparing our flux rates to those found in Fig. 1.1 (for small energies), we can assess how consistent our data is with professional systems.

This paper is broken up into several sections for ease of reading. Chapter 2 details useful information surrounding fireballs, their importance, existing research, and the theory necessary to calculate flux rates.

2 Background

Thanks to a protective atmosphere, Earth can withstand impacts from dust to boulder-sized objects traveling faster than bullets without so much as a dent on Earth's surface. While most of these near-Earth objects are extremely small and don't leave much of a trace, the larger objects can leave a trail of light visible from Earth's surface as they burn up in our atmosphere. In this chapter, we will discuss the classification of near-Earth objects, how fireballs are observed, and give important insight as to why and how we will compare our photometric survey with others.

2.1 Description of Fireballs

When considering types of near-Earth objects, many names come to mind: asteroids, meteors, meteorites, and fireballs are all often used interchangeably. However, there are several key distinctions between these objects. Asteroids are the largest of this group and are generally over 10 m in diameter [12]. These objects are responsible for massive craters that are visibly present on the moon. Meteoroids are anywhere between 10 µm and 10 m and are far more numerous than their asteroid cousins.

Meteoroids that pass through Earth's atmosphere become meteors. As a meteor passes through our atmosphere, it begins to ablate. Ablation begins when a fast moving meteor, typically traveling over 10 m/s, encounters air particles that slow it down. This leftover kinetic energy is turned into heat and is hot enough to vaporize outer layers of the meteor. Atoms within these vaporized outer layers and nearby air molecules get excited to a point where they release light. The amount of light that reaches an observer on Earth's surface can be measured in terms of apparent magnitude. Magnitude is represented on a $\log_{10}$ scale where dimmer objects are represented by high numbers and brighter objects are lower. The equation for calibrated magnitude is

$$m = -2.5 \log_{10}(I/I_0)$$

where I is the intensity of the meteor/fireball and I_0 is the intensity of a reference location. Both intensity measurements are in units of $\mathrm{W/m^2}$. Meteors with an apparent magnitude below -4 qualify as bolides, or fireballs. For reference, in it's brightest phase, Venus is a magnitude -4.4 planet while the dimmer Jupiter has a magnitude of -2.1 [10]. If an object is massive enough to withstand the pressures of Earth's atmosphere and make it to the surface of Earth, it is classified as a meteorite. These are extremely rare, occurring less than 200 times per year. Because meteorites are essentially rock remnants, they provide valuable information about the initial asteroid's origins. While there is some overlap between asteroids, meteoroids, meteors, fireballs, and meteorites, their definitions are important to distinguish. Figure 2.1 summarizes the relationship between these 5 terms.

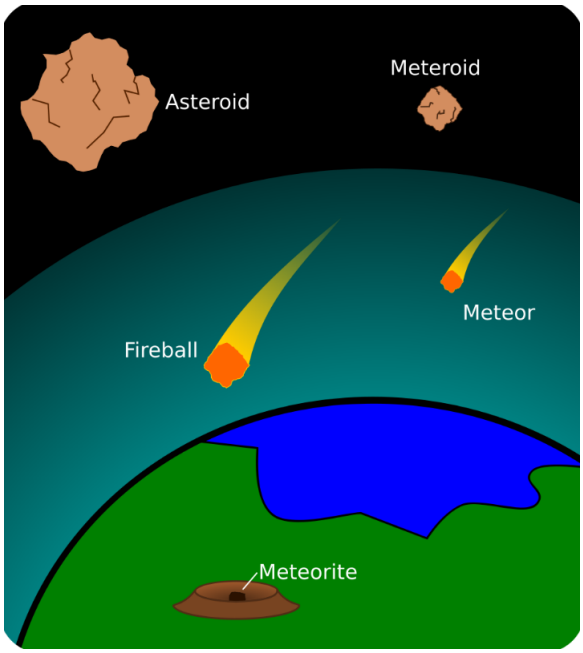

Figure 2.1: A depiction of near-Earth object classification. Asteroids and meteoroids may be found in space, while meteors and their brighter counterpart, fireballs, burn up through Earth's atmosphere. Unlike ordinary fireballs, meteorites remain intact

Our project specifically focuses on fireballs. A fireball passing through the sky is referred to as a fireball event, and these events will provide data for our fireball catalog. We may further classify fireball events into two categories: sporadic events and meteor shower events. Meteor showers occur when Earth's orbit crosses

paths with the orbit of a collection of debris. Such collections often orbit large masses such as Jupiter or the sun [13]. For example, the Perseid meteor shower has a highly elliptical orbit around the sun as seen in Figure 2.2. As comets travel through space, small bits of rock and ice separate from them. This process is due to differences in pressures and heat on different areas of the comet. Comet fragments make up a majority of the substance in meteor showers.

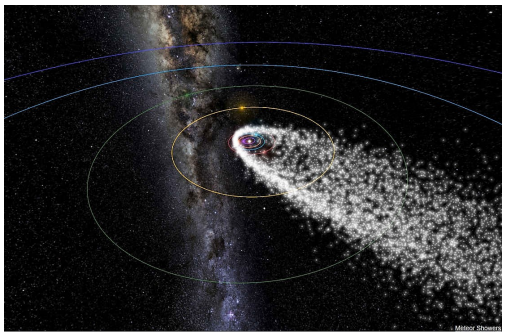

Figure 2.2: The Perseid meteor shower and its relation to our solar system.

In contrast, there is debris in space that is not connected to any meteor shower. Events stemming from random debris are called sporadic events. Due to the innate nature of gravity, debris in space often gets collected and becomes part of a larger system such as a meteor shower. Thus, sporadic events are less common. Collecting information on fireball events allows astronomy researchers to develop a better understanding of the presence of matter in space.

2.2 Event Detection

To compare our camera system to other professional systems, we must acquire enough event data to determine a flux rate. This section will discuss how different observation systems collect data on fireballs. We will specifically detail how the Willamette D6 allsky camera differs from professional cameras.

2.2.1 Existing Surveys

While amateur astronomers and low-budget systems capture useful information, larger professional systems act as a vitally important comparison point. Because many professional surveys are composed of multiple cameras working in unison, they have the advantage of multiple perspectives on a singular event. This leads to more precise measurements of parameters like velocity, apparent magnitude, and location. Individual events captured by an individual observer do contribute

to the pursuit of knowledge. However, a small camera system that cannot yield similar data to more professional surveys serves only a marginal amount of utility.

Cameras for allsky Meteor Surveillance (CAMS), the SPanish Meteor Network (SPMN), NASA's allsky Fireball Network and the Lincoln Near Earth Asteroid Research (LINEAR) program are examples of well-established existing meteor observing surveys. All of these programs are continuously acquiring data and adding their findings to existing databases. Much of this data is widely available online, but vary from survey to survey. Funded by NASA, Cameras for allsky Meteor Surveillance (CAMS) aims to verify minor meteor showers and trace them back to their existing parent comets [6]. The project was created by Peter Jenniskens and is based in California. The CAMS network is spread across 3 different locations as seen in Fig. 2.3 and consists of over 60 cameras. Each camera is has a relatively narrow field of view 30 deg. When arranged intentionally, these cameras provide a high resolution image of the entire visible sky. By spreading their cameras across three separate locations, the CAMS research group can measure precise trajectories of incoming meteors.

Figure 2.3: The three CAMS network stations within a 50 mile radius.

Similarly to the phenomena of trying to catch a baseball with only one eye open, confidently capturing a three dimensional trajectory of a fireball is extremely difficult when using only one camera. Multiple cameras provide different fireball-path perspectives and allow us to geometrically solve for the event's depth. Accurate trajectories are particularly useful in back-tracing the motion of the meteor's orbit. The CAMS team has reduced over $320,000$ of these orbits [9]

The SPanish Meteor Network (SPMN) works extremely similarly to the CAMS project. It consists of 25 observation stations located across Portugal and Spain [13]. In addition to becoming the first organization in Spain to successfully calculate the orbital path of a meteor, this organization revolutionized fireball research

by developing the first CCD allsky cameras, or cameras that observe the entire visible sky. [7] While this approach results in lower resolution event capturing, it is much cheaper and covers the same sky area. These cameras are now in use all across the world.

While the SPMN and CAMS are extremely powerful research organizations, their study of meteors only slightly overlaps with the research being discussed in this paper. Because of their high grade equipment, they are able to capture data from extremely dim sources. Fireballs, quantified by a magnitude below -4, compose only a small fraction of the meteors analyzed by these organizations. Fortunately, other organizations focus specifically on larger and brighter events.

There are a multitude of ways that one can attain information about a fireball. All the aforementioned surveys have employed the use of photometric data. In contrast, Peter Brown took data from the Department of Defense and the Department of Energy space-based systems in geostationary orbits. The original purpose of these systems is to detect signatures of explosions near Earth's surface, but the system occasionally picks up false positives in the form of ablating bolides. Because the systems detect the amount of power released, Brown and others have used the systems to approximate a fireball's energy. In a 2002 article published by *Nature*, Brown estimated the optical energies of around 300 bolides. Drawing from this data set and other existing data sets, Brown created compiled the following equation which relates bolide energy to the number of impacts on Earth each year.

$$\log N = a_0 - b_0 \log E \tag{2.1}$$

where N is the total number of objects colliding with earth each year and E is the respective energy of the sample in kilotons [2]. In this empirically derived equation, $a_0 = 0.5677 \pm 0.015$ while $b_0 = 0.90 \pm 0.03$. This relationship is known as a power law and will be useful to compare our Willamette D6 allsky data with.

2.2.2 The D6 Allsky Camera

The Willamette University D6 allsky camera was created in 2016 to capture images of fireballs streaking through the night sky. The aim of the project was to create an economically feasible and highly mobile observational system. The Willamette D6 allsky camera was constructed by Kyle McSwain alongside Dr. Jed Rembold in 2006. It is composed of a portable structure surrounding a state-of-the-art camera system along with necessary supporting devices, including a controlling Raspberry Pi. [8]. The assembly resembles a Star Wars astromech droid, and acquired its name from this inspiration. The enclosure with visible camera is shown in Fig. 2.4. The D6 allsky camera is currently operational and has been gathering data

since the summer of 2018. Below, we will discuss the design of the D6 allsky camera while also highlighting what makes it significant.

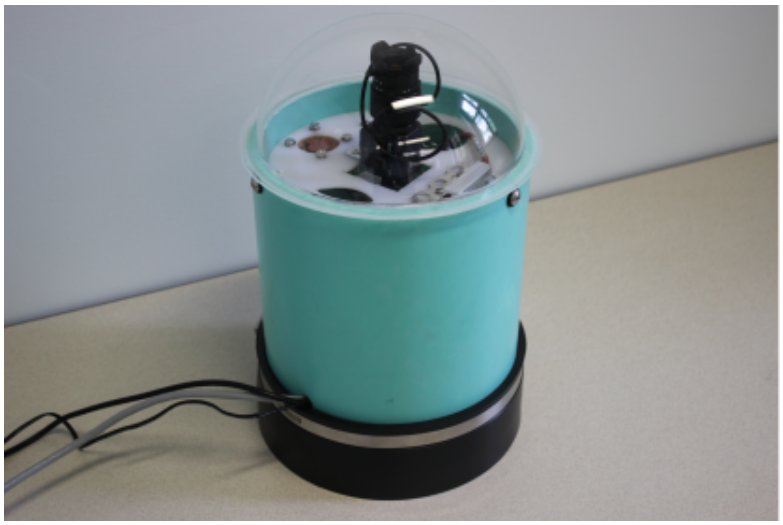

Figure 2.4: The Willamette D6 allsky camera (2016). Paired with a little imagination it resembles an astromech droid from Star Wars.[**We should get a new image of this, as it has the sealing cowl along the top now.**]

The components of the D6 allsky camera are comprised primarily of 5 different pieces: the camera housing, a CCD camera, a thermostat, a digitizer, and the Raspberry Pi to control everything. The acrylic dome and PVC shell form the exterior of our system. The dome itself is a transparent half sphere that sits on top of a PVC cylinder that holds the system together. Both act as a protective layer between the sensitive inside components and the outside environment. Without this feature, the system would be subject to rain, snow, dew, bug contamination, and other undesired effects.

The CCD camera is perhaps the most important feature of the system. The Watec 902H2 CCD camera uses a fish-eye lens to observe the entire visible night sky. It was chosen due to its extremely high sensitivity and resolution [14]. However, it should be noted that more expensive systems consisting of multiple cameras (like CAMS) provide an even higher resolution of fireball events.

Because of its constant use throughout the night, the system itself can get very warm and therefore needs some thermal regulation. The inside components are kept at a relatively constant temperature above the dew point by a thermostat and a fan system. The camera outputs an analog signal which requires the use of a digitizer before it can be processed by the Raspberry Pi. The coaxial signal is sent to the digitizer before connecting to the Raspberry Pi via USB.

While there are several similarities in the composition of our allsky camera to existing systems, there are several key differences. The most prominent of these

are the size, versatility, and cost of our system. Around the size of a basketball, the D6 allsky camera is extremely compact. Not only is it small, but it only relies on a single power chord for power. Because of this, the camera can be easily picked up and relocated to any setting that has a power source. The system has low power requirements and it should be possible to run from a battery if remote placement is desirable in the future. Other systems, such as several CAMS camera setups are rooted to extremely powerful computers that have little to no mobility as shown in Fig. 2.5.

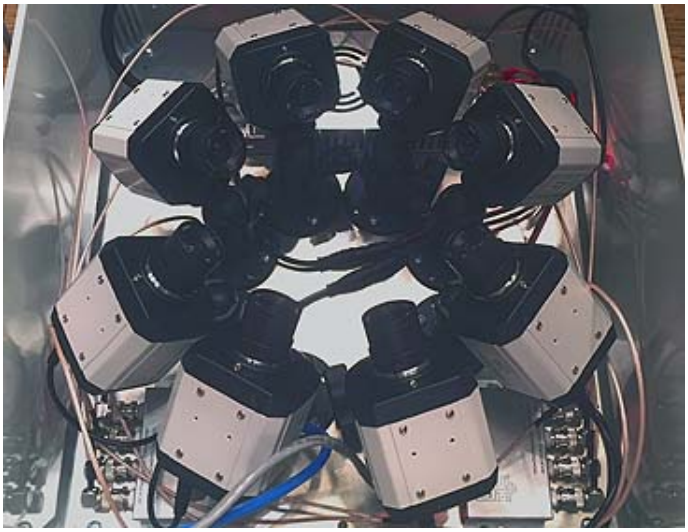

Figure 2.5: An entrenched alternative fireball observation system.

This presents issues related to being rooted in one location such as building renovation or sporadic light pollution issues. For example, if a tree were to grow near the camera, it would need to be chopped down or the entire system may need to be relocated. With the lightweight and portable D6 allsky camera, relocation is not a difficult process.

Additionally, the D6 allsky camera is a less expensive alternative to other fireball analysis tools. The ingenuity of running initial analysis on a microcomputer allows the D6 allsky camera to cost a fraction of what professional systems cost. Although large professional organizations produce copious amounts of wonderful data, in the field of fireball research, amateur systems outnumber professional systems 2 : 1 [3]. Providing a cost efficient alternative could be a great way to expand the field of fireball research and in turn provide a better understanding of the near-Earth objects in our solar system.

2.3 Photometry

After collecting videos of potential fireballs, next comes the task of analyzing the videos. Luke Russell, advised by Dr. Jed Rembold, wrote a photometry program in Python that allows us to get a calibrated light curve for a given video of a fireball. Simply running a fireball video through his interactive GUI allows us to access information about luminous properties of the fireball. However, limitations to our photometry must be taken into account. False positives, extinction, and other error factors must be accounted and corrected for while creating our fireball catalog.

2.3.1 Existing photometry tools

The primary photometric analysis tool that we use is a Photometry GUI in which a user interacts with a fireball video. After selecting both of these and entering in the known magnitude of the reference star, our photometry program automatically tracks the fireball throughout the following frames. By using Gaussian fits to the photometric data, the program is able to center its view on the fireball and determine its size throughout its path. Throughout this process, the video also sums the photon counts for each fireball pixel for each frame. This photon count gives us the magnitude of the fireball at a given point in its path. Doing this for each frame results in a light curve that shows the magnitude as a function of time, which yields the valuable light curve. From this light curve, we can then move on to further analysis.

2.3.2 False Positives and Atmospheric Extinction

While it is able to capture fireballs, the D6 AllSky camera still picks up a great deal of false positives. In an initial sample of over 700 videos, only 2 of them contained real events. The vast majority of the videos were of bugs crawling across the acrylic dome. Because the bugs are illuminated by nearby light, they appear to be bright spots traveling across the screen and thus the detection script mistakenly flags them as fireball events. Moreover, many bugs are featured in several videos as they have a tendency to move, stop somewhere, and move again. While this is somewhat problematic, we aim to implement several steps to limit the number of false positive bug cases. We aim to implement video length restrictions, and linear motion restrictions to limit the number of false positives.

In addition to bugs, other events such as airplanes, satellites, and Iridium flares provide false-positive videos. Their near-linear motion and bright presence are an instant trigger for the fireball detection. A larger problem in data analysis stems from the phenomena of atmospheric extinction. As shown in Figure 2.6, we

observe that when looking close to the horizon, light must travel through a larger volume of atmosphere than it does for an observation close to the zenith. Because the light travels through more atmosphere, more of the light is absorbed by gases or scattered by air particulates [5].

Figure 2.6: A depiction of atmospheric extinction's effect on a sunset on a smokey day.

Part of this project will include accounting for atmospheric extinction in a secondary photometric analysis script. This will involve measuring the light intensity of known reference stars at various pixel locations throughout the night and comparing them to the real intensity values. This will allow us to have calibration values for different pixel locations throughout our camera's frames, and thus will be applicable to any event's analysis.

2.4 Parameters of Interest

As previously mentioned, the most critical component of our analysis is the final measured flux of our system. To recreate a plot similar to Fig. 1.1, we must have multiple events, estimated energies/masses of each event, total area of sky covered, and the total observation time. This section will detail how we will go about collecting this information.

2.4.1 Fireball Mass and Energy

Because of the limitations of using one camera system, we will make several key assumptions in determining any fireball's initial mass and energy. Firstly, we

assume the velocity of the fireball. This will vary depending on the associated meteor shower. Additionally, we will assume a luminous efficiency, τ, on a similar basis. The following equation can be used to determine the optical energy of a fireball.

$$\tau = (0.1212 \pm 0.0043) E_0^{0.115 \pm 0.075}$$

Optical energy is useful, as it proved us a relationship to total fireball energy through the following equation.

$$E = 8.2508(E_0)^0.885$$

This is an empirically derived formula based on data taken by Peter Brown [2]. Now that we have a clear image of how to determine energy, we can transition to finding the initial mass of a given event. To do this, we will need the mass and radius of the fireball.

Paired with our assumption that fireballs on average have a density of _____ and a generally spherical shape, we can calculate the diameter using the following equation,

$$d = 2(\frac{3m}{4\pi\rho})^{1/3}$$

where ρ represents the density of the fireball prior to entering the atmosphere. [1]

The light curve outputted by our existing photometry GUI allows gives us light intensity at any given time. The luminosity is then related to the intensity of the fireball through the following formula,

$$I = \frac{L}{4\pi r^2}$$

where I is the intensity, L is the luminosity, and r is the radius of the object in question. The radius is easily attainable from the diameter. This luminosity will help us estimate the initial mass of the object in question. Equation 2.2 can be used to determine the initial mass of an ablating meteor,

$$m = \int \frac{2L}{\tau v^2} dt \tag{2.2}$$

where L is the luminosity, dt is the change in time, v is velocity, and tau is the luminous efficiency.

[1] I will definately still need help in this section

2.4.2 Time Observed

Each individual video or night snapshot taken by the Willamette D6 allsky camera is labeled with a time stamp. In addition to this useful time documentation, when operating, our allsky camera has a running log of its functions. This well-kept documentation allows us to keep track of the total observation time, a critical component of determining flux. However, there are certain limitations associated with the amount of time we can observe.

Primarily taking data in Salem, Oregon, the Willamette D6 allsky camera is subject to weather in the pacific northwest. Rain and cloudy nights limit the number of days we may take data. Luckily, the versatility of the camera system allows for it to be taken to alternative locations during school breaks or periods of bad weather.

2.4.3 Total Observation Area

One factor that is particularly difficult to deal with when considering flux is the area of the sky that is being observed at a given time. Using basic trigonometry, we can work out that:

$$\text{Sky Coverage} = \Omega(h + r)^2 \tag{2.3}$$

where Ω is the steradian, or solid angle from earth, h is the height above Earth's surface, and r is the radius of Earth. We will get a concrete steradian value by comparing angular distance to pixel distance in our camera frames. To expand on this, when a moon travels through the night's sky, it covers a angular distance in the sky. If it were to travel from one horizon directly through the zenith to the other horizon, it would have traveled an angular distance of 180 deg. If we know the angular distance traveled and the total number of pixels traversed, we can establish a relationship between the two and get a precise steradian value. Plugging this value into Eq. 2.3 yields a sky coverage area.

One might naively assume that the total observation area would remain consistent each night. However, one must consider clouds and fog when calculating the overall sky area covered. This consideration will be dealt with in our secondary analysis and is further discussed in the methods section. ’

3 Methodology

To calculate the flux of fireballs from our D6 AllSky Camera, we need to find the total observation area, time, and the total number of events. In this section, we ~~will describe~~ begin by describing in detail our methods for finding each of these properties. ~~We have considered and will discuss~~ Some time will be spend discussing obstacles such as camera fish-eye effect and cloud interference. Additionally, we will delve into the structure of our database~~, the~~ : our fundamental tool for secondary statistical analysis.

3.1 Calculating Total Observation Time

Each night the D6 AllSky camera ~~is placed outside to observe, the Raspberry Pi, the computer behind our observations, runs a program that outputs~~ observes, a program is run on the controlling Raspberry Pi that logs important information throughout the night. ~~This output takes on the form of an observation log.~~ The observation log is a simple time-stamped text file that records what processes the ~~camera~~ system runs at various times in a given night. ~~To provide examples~~For instance, the observation log ~~states~~ contains when each observation run begins (when the camera is set up initially), when the camera begins its analysis, when a new event is detected, and when the analysis goes to sleep, along with ~~many other useful bits of information~~potential warnings or error messages that might come up.

To calculate the total observation time, we ~~can~~ run a Python script that searches for the time associated with ~~a new analysisbeginning~~the start of each new analysis. After this time is recorded, we ~~may~~ continue down the list of information until we find the time associated with that ~~analysis'~~observation run's end. By subtracting the two times, we ~~have found~~ find the total observation time for that specific night~~of camera analysis~~. Performing this same method in a loop throughout all of the nights allows us to find how much time we spent observing

on a given night. By summing up the total time observed over each night, we can attain the total observation time over the course of our data collection period.

A depiction of a ~~simplified~~ portion of an observation log and our time analysis table can be seen in ~~Fig.~~ Figure 3.1. Note that while the information row that contains "New Observation Run Started" sounds as if it represents the start time, we define our start time from the information row that states "A new night has arrived! Frame analysis beginning!".[1] End times are determined by the information rows labeled "Day has come. Analysis going to sleep."

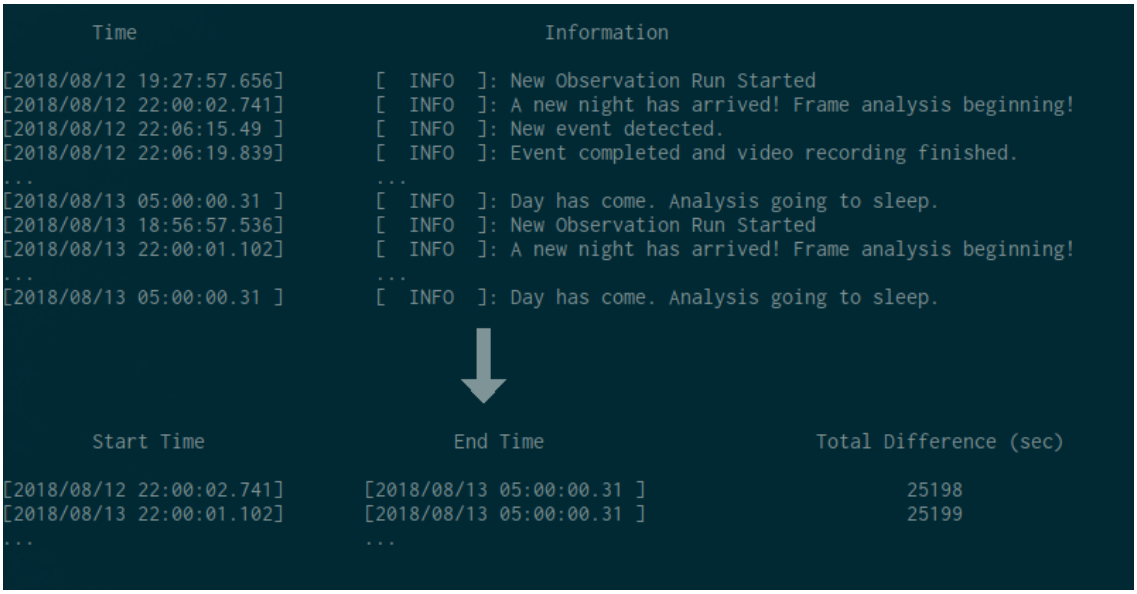

Figure 3.1: An example observation log and the resulting time analysis information

It is imperative that we save not only the total observing time over a given night, but also the start and end times. [2] This information is crucial for the next section, ~~Calculating Total Observable Area~~where we calculate the area of sky observed on a given night.

3.2 Calculating Total Observation Area

One of the most difficult problems we needed to address for this project was determining ~~the~~ what area of the sky the D6 AllSky Camera ~~'s observation area~~observed each night. In an ideal world, our camera would be able to see all parts of the

[1] Should comment on why this is.

[2] Is it important to comment about errors you find when doing this matching? Or if you throw away tiny portions where the camera was clearly being tested?

observable night sky, spanning across all horizons. However, due to ~~photometric~~ optical limitations of our system ~~(and that of most systems)~~and fisheye lens, this is not possible. ~~Because determining a flux ,~~ Nevertheless, determining the flux is a primary goal of this project, and is directly dependent on observation area~~,~~ . As such it is vital we come up with a means to get a precise estimate~~.~~ [3]. [**In this paragraph you were mainly focusing on the issue of us not getting the entire circle within our field-of-view, correct? Might want an image to better illustrate that.**]

To make matters more complicated, ~~our AllSky camera experiences significant fish-eye effects. A fish-eye effect refers to the distortion of an imageas you travel further from the azimuth~~ while the use of a fisheye lens gets us more coverage of the sky, it also results in some distortion of the image. These distortions generally get worse the further an object is from is from zenith (directly overhead). ~~For~~ An an example, imagine a square cloud located directly overhead. As that square drifts towards any given horizon, its size becomes smaller relative to you, the observer.[4] The significance of this problem as related to our project stems from the fact that while 50% of our camera's pixels may be covered by clouds, this doesn't necessarily mean that 50% of the observable sky is covered.[5] Therefore, we need some way of relating a given camera region to some observable distance.

To do this, we used observations of the ~~moon and~~ Moon and various stars to calculate angular distance to pixel ratios for different regions of our camera. This solution addresses the need to account for a camera fish-eye effect by assigning different ~~regions of view to different~~ fields-of-view to different pixel observational areas. By ~~assigning~~ correlating certain pixels with specific angular ~~distance ratios~~distances, we can analyze the ~~sky coverage of clouds spanning different camera regions~~available sky coverage by summing across all pixels. To fully understand the methodology behind calculating the total observation area, one must understand how angular separation serves a role in area coverage.

3.2.1 Angular Separation

Consider two objects, both of which are visible to you, an observer. One simple way to compare the two objects is by measuring the direct distance between them. ~~A slightly more complicated~~ An alternative way to compare the two would be to imagine two straight lines extending from your ~~line of sight~~ location to both objects. Because both lines are extending from the same location, we can calculate the associated angle between the two ~~objects~~lines, known as the angular separation. This angular separation may change as you move locations if the

[3] This seems a bit of a paradox...

[4] Probably need more evidence or argument than this.

[5] good, and well put.

objects are nearby. However, if both objects are extremely far away, no small change in observer location will change the angular separation significantly.[6]

We can apply this concept and principle to calculating angular distances between stars and other celestial objects. By finding the angular separation across a given pixel, we attain a precise estimate[7] for angular coverage of the camera.[8] Assuming that the fireballs are ~~passing through~~ ablating in our atmosphere at a given height, we can then apply our angular measurements to attain an observational surface area as desired. It is easy to imagine this surface area used in flux calculations as the base of a cone, where the cone's point represents the viewer's field of view.[9] Importantly,to calculate angular separation between objects, we need to first have a database of objects to compare.[10]

[**I think you need to revisit the idea that you want to use the known positions of stars and the Moon to serve as these calibration points before jumping into the next section.**]

3.2.2 Collecting a Star Catalog

While the primary aim of the D6 AllSky Camera is to capture video footage of fireballs, it serves many other roles.[11] Throughout the night, it takes several snapshots of the nights sky. The motivation behind this is primarily to ~~recognize~~ check cloud coverage, but these images can store other important information.

Stars are visible in many D6 AllSky Camera's snapshots. The first step in creating a catalog of star information is recognizing stars within snapshots. We went about this by cleaning the image of hot spots, ~~then enacting a threshold~~thresholding the image, and using the ~~function~~ a `SimpleBlobDetector` to capture star locations. All of these processes are ~~performed using~~ coded and executed in Python.

Hot Pixels and the Dark Frame

Hot pixels are flawed pixels within a camera that always provide a significant positive photon count, even when the camera is exposed to complete darkness. These pixels are problematic when trying to locate stars, as they don't represent

[6] We use angular separation because we have no idea what radial distance separates the objects (generally). As such, we treat everything as being an equal radial distance away, and hence get the concept of the celestial sphere. And angles are a natural way to measure displacement on a sphere.

[7] this again

[8] only if we sum over all the pixels

[9] But it is a rounded cone?

[10] You really need a picture or pictures in this section.

[11] This feels a bit awkward to me. It does these other things in an effort to better describe the population of fireballs.

any real physical object. Fortunately, this source of error can be accounted for by taking an image while the lens of a camera is covered. This is called a dark frame, because the lens is not exposed to light. ~~The~~ Ideally the dark frame displays a black image, ~~with a few exceptions, the~~ but most cameras will have a few hot pixels. By subtracting this dark frame, represented by a 2-dimensional array of values ranging from 0 to 255, we are able to remove the hot pixel's effect from all other frames.[12]

Thresholding

Once these hot pixels are subtracted from a given frame of interest, the next step is to enact some type of threshold. In this case, a threshold represents a cutoff photon count[13] for every pixel. If a pixel has a count that is lower than the threshold, that photon count is changed to zero, ~~or~~ which is pure black. Alternatively, if a pixel has a count that is higher, the count becomes 255, or pure white. ~~Threshold~~ Thresholding serves the important role of ~~reducing or~~ simplifying an image ~~. They~~ to a purely black and white, on or off type image. It also remove some of the inherent error associated with photon counts.~~For the purposes of this project, we used an initial threshold of 140.~~ [14] The necessary threshold for different images differed in accordance with the amount of surrounding light. ~~Because of this , if~~ For the purposes of this project, we used an initial threshold of 140. If 140 was not a sufficient threshold, ~~we increased this value~~ this value was increased in increments of 5 until the resulting image appeared ~~properly reduced~~to properly segment between open sky and clouds. For example, images that contained the ~~moon, a source thats pixels' photon counts bleed into~~ Moon, a bright source that tends to wash out neighboring pixels, needed higher threshold values than images without.[15]

SimpleBlobDetector and Stellarium

Next, we use the `SimpleBlobDetector` function from the `CV2` library to detect potential stars. This function is able to read an image and scan for objects that meet your specified parameters. Variable parameters include, but are not limited to, size (in pixels), circularity, convexity, and color. In this instance, the color has a value of 255.[16] When enacted, this function scans the picture and returns a list

[12] An example would be nice.

[13] Careful calling these photon counts. They are related but not directly proportional. Better to just call it pixel brightness.

[14] How are you justifying this? Or what do you mean?

[15] I'd like to see some images illustrating this here as well.

[16] What about those other parameters?

of detected locations centered on the object. Using simple plotting functions, we can overlay these locations with the original image.

At this point, we have a list of potential object locations, but no foreseeable way of identifying the real ones. As luck would have it, *Stellarium*, a free astronomy software allows users to view a clear night sky from any point on earth at any time. Additionally, this interactive software stores information about the stars' names and other important information. By viewing *Stellarium* and a D6 AllSky Snapshot and comparing the two, we are able to recognize which objects are real and which are false positives.[17] Because each snapshot is labeled with the corresponding data and time, this method proved sufficient in identifying celestial objects from images.

~~A D6 AllSky snapshot (left) alongside a Stellarium display (right)~~

A depiction of this process can be seen in ~~Fig.~~ Figure 3.2. When comparing the two images, it should be clear that the ~~values~~ objects numbered 17, 16, 19, and 21 correspond to Betelgeuse, Aldebaran, Capella, and Polaris. Also note that in the image, there are several recognized objects that don't have any celestial counterpart. These are all false positives. Similarly, there are cases in which the `SimpleBlobDetector` is not able to recognize an object that appears in a snapshot.

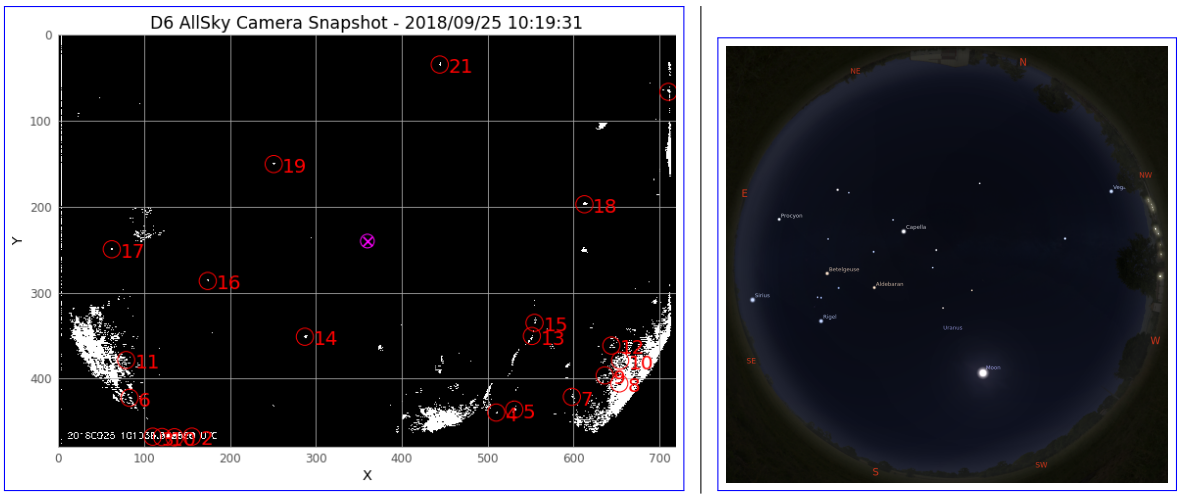

Figure 3.2: A D6 AllSky snapshot (left) alongside a Stellarium display (right)[**Please fix this image so the dark regions of the images align! Also, you need a much more robust caption explaining what is happening in each image. And you might want to zoom into Stellarium so its field-of-view roughly matches that of the image?**]

Once an object in a given frame ~~was matched to it's~~ is matched to a name,

[17] "Why are there false positives? I thought we eliminates the hot spots?"

we used the coding library `Vizier`[18] to automatically look up the star's right ascension, declination, V-magnitude, azimuth, and elevation. This, combined with the star's pixel location, time, and reference file name[19], was added to our star catalog as a singular data row.

Azimuth and Elevation

Each star has several inherent properties such as magnitude, right ascension, and declination. The later two represent coordinates that ~~can help locate the star~~ locate a star on the celestial sphere. Other properties, such as a star's azimuth and elevation change over time and vary dependent on the observers location. These two properties indicate a star's position in the sky relative to an observer and act similarly to spherical coordinates.[20]

Through finding the azimuth and elevation of a star, we can assign a star a 3-D coordinate value that lays on a unit sphere. ~~Using some clever algebra, we can~~ Wwe can then calculate the angular separation between two 3-D coordinates ~~. A principle of any dot productstates that~~by taking advantage of properties of the dot product:

$$\vec{A} \cdot \vec{B} = |\vec{A}||\vec{B}| \cos(\theta)$$

where θ represents the angular separation between the two unit vectors. Because we know that both vectors representing star locations will fall on a unit sphere, their magnitude is 1. Using this knowledge, we may transform the above equation to:

$$\theta = \arccos(\vec{A} \cdot \vec{B})$$

Given this formula along with information stored in the star catalog, we are able to calculate angular distance per pixel across different regions of the camera frame.[21]

3.2.3 Calculating Angular Areas

The D6 AllSky camera is a versatile system ~~that~~and it's orientation can change slightly from night to night. Because of this, there are several considerations

[18] I'm actually not familiar with this. Is this a standard Python library or part of AstroPy?

[19] What is this "reference file name"?

[20] You really should comment or provide an image of what each one measures!

[21] Whoa, this is a jump. With this you can just calculate the angular separation between two points that we happen to see in our image.

that must be accounted for when calculating angular distance per pixel across different camera regions. For example, if pixel $(10, 10)$ has an angular separation per pixel of 0.10 one night, if the camera rotates by 45 deg we may read a different angular separation per pixel at that location. [22] This is because the pixels may be representing a different area of sky upon rotation. We have developed a method to account for this consideration.

Comparing Objects from the same Night

The star catalog stores information about celestial objects over the course of all observations. Using constraints from the Time Analysis information (start time, end time, time elapsed), we can isolate rows within the star catalog from a specific night. After creating this subsection, we can then use our described method to calculate the angular separation per pixel for every combination of two objects.[23] One might question where the data behind this angular distance per pixel should be located. After all, there are two different object locations used to calculate the value. Our strategy was to locate the point in between the two objects. Figure 3.3 depicts these combinations along with the locations of the angular separation per pixel represented as white dots.

Figure 3.3 gives a general depiction of our method on a much smaller scale. Note that when comparing objects from this subsection of the star catalog, we are not limited to only comparing different stars. As an object moves throughout the night sky, its azimuth and elevation change along with its pixel location. ~~That being said, we can~~ We can thus treat each individual ~~row and~~ observation as a unique object, ~~creating~~ even comparing between the same object at different times throughout the night. This creates many more combinations than if we were to only consider unique stars.

After calculating all potential angular separation per pixel values alongside their location information, we may move on to calculating average angular separation per pixel in different camera regions. For the sake of simplicity and practicality, we split up our 720×480 pixel camera frame into 40×40 pixel squares.[24] All angular separation per pixel measurements located inside a given square were averaged over to determine that square's value. Figure~~4.3~~ 3.4 shows the resulting average angular separation per pixel for different squares in our camera frame.[25]

---

[22] Should we though? Wouldn't the argument be that the camera should at least be rotationally symmetric?

[23] I'm confused. I don't feel like you have made clear how this angular separation per pixel is calculated yet?

[24] From a coding point of view, this wasn't really necessary. Why did we really do it?

[25] Given your comment in the code. Is this the final version or the version that still needs fixed?

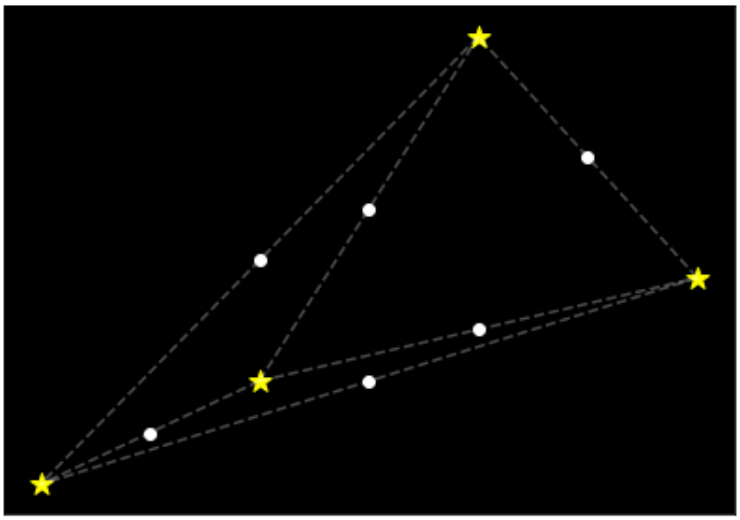

Figure 3.3: A simplified depiction of angular distance per pixel locations[Clarify what you mean by this.] (white dots) given a set of objects (yellow stars).

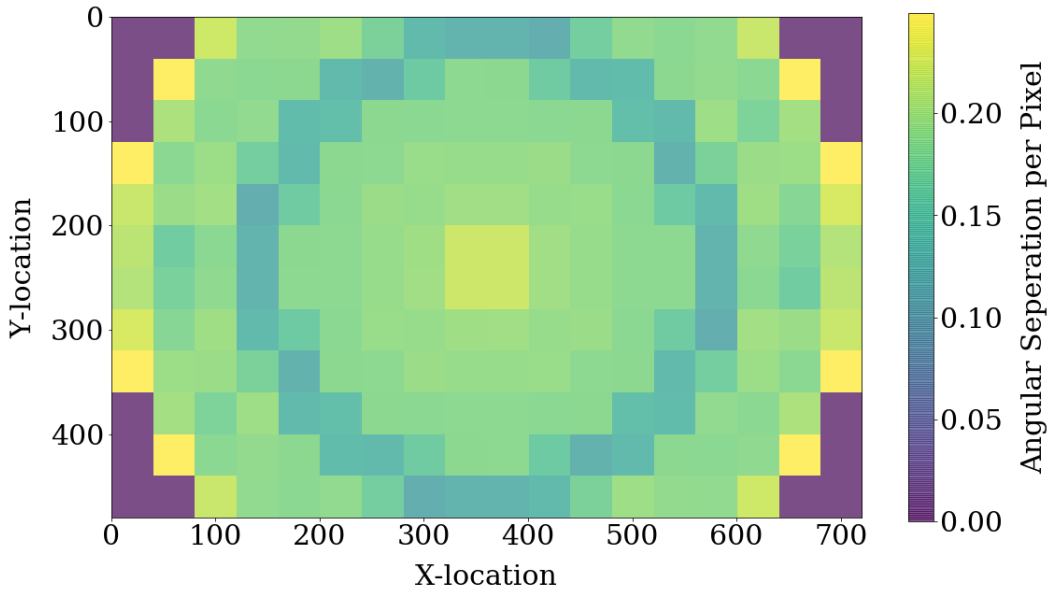

Figure 3.4: Average angular separation per pixel for different camera regions. [Again, you need more robust figure captions. Also, did you ever talk about rotating the points?]

3.3 Calculating Cloud Coverage

The D6 AllSky Camera does not always remain outside. For the protection of the system as well as for saving power purposes, the camera is only placed outside

during nights where observation conditions are promising.[26] Some nights, the sky is clear throughout the entire night, while others are partially cloudy.[27] Because we cannot see or properly analyze fireball events that happen behind clouds, we cannot count cloudy regions as observable areas. As mentioned previously, the D6 AllSky Camera takes several snapshots of the night sky systematically throughout an observing session. Specifically, it currently takes images every 30 minutes. By using ~~simple~~ thresholding, we have seen how we can determine which pixels qualify as not observable areas. The threshold value that we used in this step was a photon value of 90.[28]

Unfortunately, some pixels that fall within a broad cloud area are not recognized through this process. The solution to this problem lies in the `CV2` functions `MORPH_CLOSE` and `MORPH_ERODE`.[29] The first of these functions ~~files~~ fills in regions of empty space that are next to filled in space. This is helpful in closing gaps between pixels that represent clouds. However, because the edges of the clouds are expanded in this process, we must subsequently perform a `MORPH_ERODE` that works in the opposite fashion. Once a hole is completely closed, there is no space within a cloud for the eroding function to open up, hence providing a satisfying answer to the cloud predicament.[30]

After this successful threshold and subsequent closing/eroding process is complete, the next step is implementing the relationships between pixels and angular distance as seen in ~~Fig. 4.3.~~ Figure 3.4. By assigning the correct regional angular separation per pixel value to each pixel within a cloud, we are able to estimate ~~its angular area covered. Figure~~the angular area that cloud covers. Figure 3.5 shows the processes taken in calculating the area occupied by clouds. Note that both a filling and eroding function was used to attain the lower left image. The observable area during that time is the cloud coverage subtracted from the total observation area.

This ~~method~~ process is performed for each snapshot. In creating our average area observed calculations, we assume that the sky retains that same amount of cloud coverage for the 15 minutes prior to and 15 minutes after the snapshot. While this isn't precise down to the exact minute, over many observations, the number of over-estimations and under-estimations should ~~cancel~~ average out and yield an accurate observational area.

---

[26] That shouldn't remain that way forever though. The intent is clearly to have it outside all the time in the end.

[27] Actually, given the direction you went with this, why even mention the above?

[28] Why does this threshold differ from the one earlier?

[29] These are more any binary image functions that CV2 specific

[30] You should reference the image earlier for a visual to better understand what you are trying to eliminate.

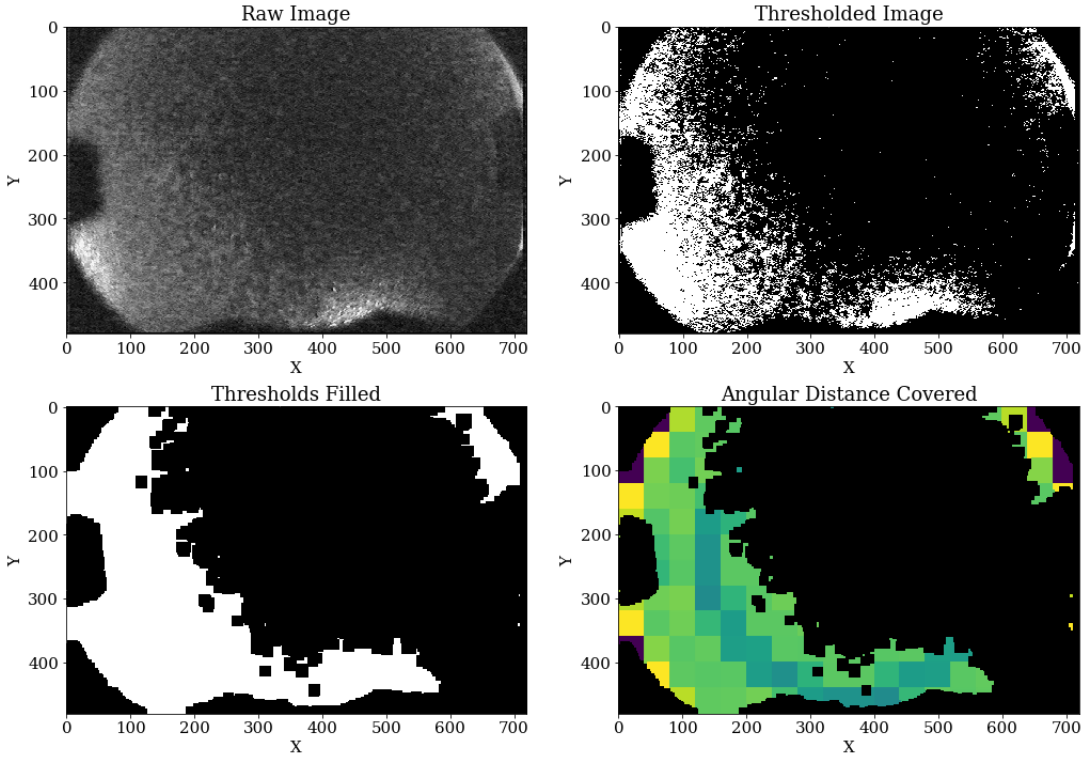

Figure 3.5: The processes behind determining the area of cloud coverage. [**Way more robust caption. This is arguably the most important image of your analysis section. Don't chince out on it!**]

4 Data

Because there is intrinsic variability in the number of near-Earth objects colliding with Earth's atmosphere from night-to-night, a sufficient data sample plays a vital role in estimating an average flux. This chapter details our data sample, specifically with respect to our time, observable area, and fireball distributions. To assess the overall capabilities of our system, we also delve into the data behind our star catalog, previously used for total observable area calculations. While this chapter provides the raw data samples and overall distributions, a further analysis and interpretation of the data can be found in Chapter 5.

4.1 Time Distributions

The D6 AllSky Camera does have a protective shell, however it is not always placed outside for nightly observations. Due to Oregon's climate, we often leave our observation system inside. There have been a total of 221 days between August 27, 2018, the beginning of Willamette's academic year, and May 6, 2019. Out of those 221 days, we have been able to observe for 34 nights, for a total of 291.87 hours.

Once placed outside to observe, the D6 AllSky Camera begins taking observation when the sky is dark enough to take videos of without fear of over-saturation. As the sky gets brighter when sunrise approaches, the camera automatically shuts off, ending the observation session. This brightness constraint means that the total observation time changes from night-to-night. We observed for an average of 8.584 hours per night. The shortest observation session lasted 7 hours while the longest lasted 11 hours.

Figure 4.1 displays the individual nights that we observed throughout the academic calendar. In addition to plotting our observation dates and that sessions total observing time, we have indicated dates of meteor showers visible in Salem, Oregon. During the months of October and November, we observed on nights of the Orionid and Leonid showers respectively.

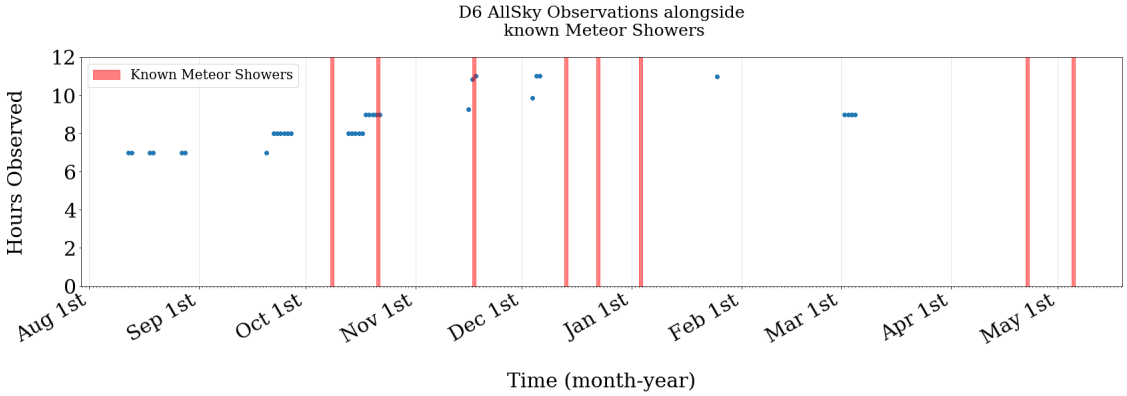

Figure 4.1: A plot of all D6 AllSky observation dates and recognized meteor showers within the $2018 - 2019$ academic calendar year.

4.2 Coverage Distributions

As described in the methodology section, to calculate the angular distance per pixel for a given location, we needed two different celestial object measurements. By taking the angular separation between the two, we designated the ratio to their respective midpoint. In total, we used 2638 comparisons to create our angular separation per pixel data-set. Figure 4.2 shows all of these points, each colored with their respective angular separation per pixel ratio.

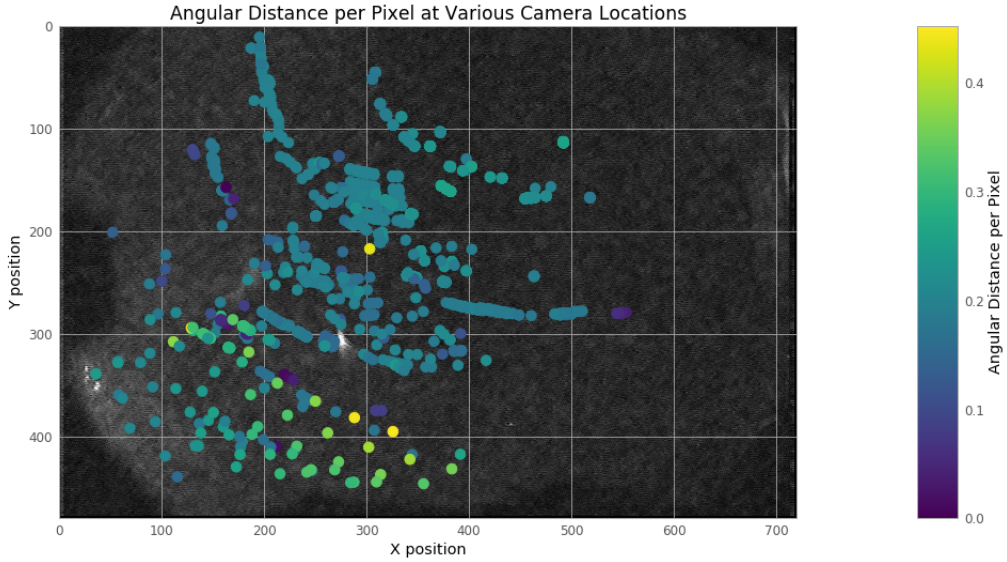

Figure 4.2: A plot of angular separation per pixel measurements from celestial comparisons.

One may note that Fig. 4.2 shows many data points, but they do not span the entirety of the camera field. There are many regions with no data points. Because has a view that is symmetric about the azimuth, we rotated all of our data points by a fixed quantity and appended them to the current data set. This assumption of azimuthal symmetry allowed us to attain a more robust data sample without sacrificing data quality. By rotating and appending in sequences of 5° in a full unit circle, we were able to increase the number of data points by a magnitude of 71.53. From this point we were able to then bin the data and create Fig. 4.3.

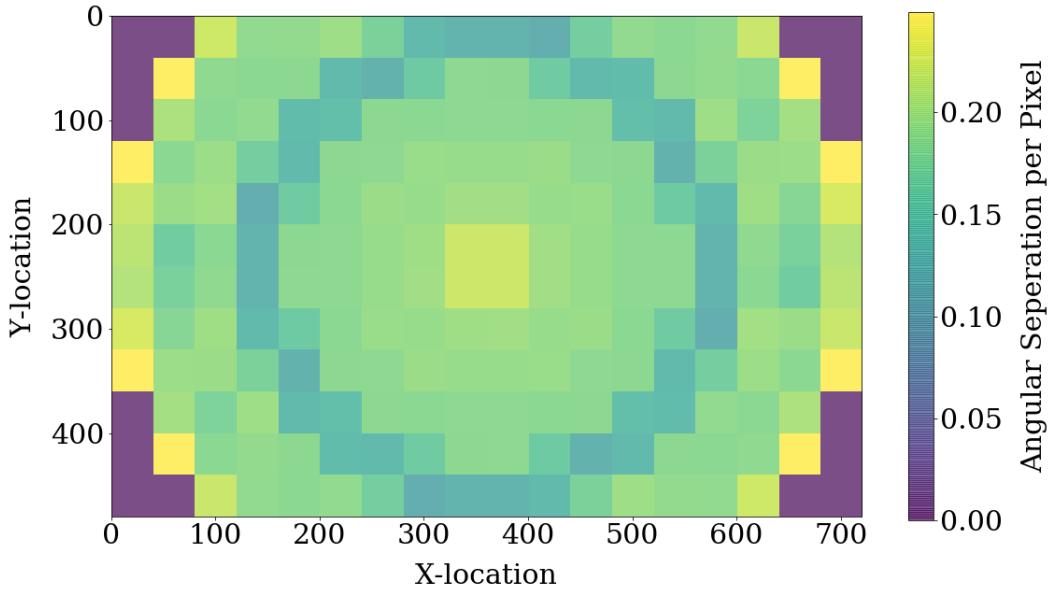

Figure 4.3: Average angular separation per pixel for different camera pixel regions.

As described in the Background chapter, we used our measured solid angles for each region to calculate individual rectangular pyramid-created sky areas at a fixed radius of 11.4 km Our measured total areal coverage was $->$ 58 974.88 km^2 $<-$.

As some nights were cloudy and others clear, the observable area value fluctuated in time. Figure 4.4 depicts both the total observation time and the average observable area for each of our observation months.

Our average observable area across all observations was $->$ 56 012.03 km^2 $<-$. This value, along with our total observation time and number of events will be used to determine the overall average flux.

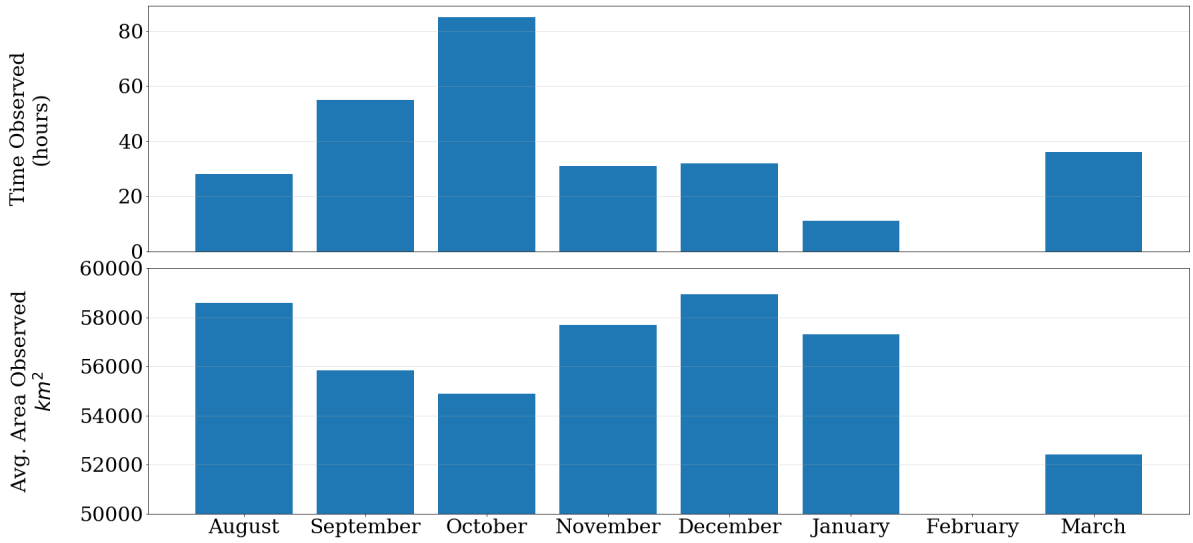

Figure 4.4: A plot of total observation time and average observable area for each month.

4.3 Detected Fireballs

In total, the D6 AllSky Camera captured a total of 1095 videos. Of those 1095, only 6 were identified as real fireballs. A depiction of the locations of these fireballs can be found in Fig. 4.5.

Of the 6 fireballs, 3 were found within 24 hours of the Leonid meteor shower while 1 more was found during the Orionid meteor shower.

Unfortunately, the GUI program used to analyze fireball properties was unable to work on each of these cases. Therefore, we will have to wait for updated data on the property distributions of our catalogued fireballs.

4.4 Camera Capacities

As described in Chapter 3, the star catalog consists of recognized stars from the D6 AllSky Camera's snapshots. In a catalog containing a total of 317 rows we observed an average of 1.396 stars per snapshot containing at least one star. In total, the system took 1642 snapshots, and 279 of them contained celestial objects (stars or the moon). Within those 227 videos, we captured information

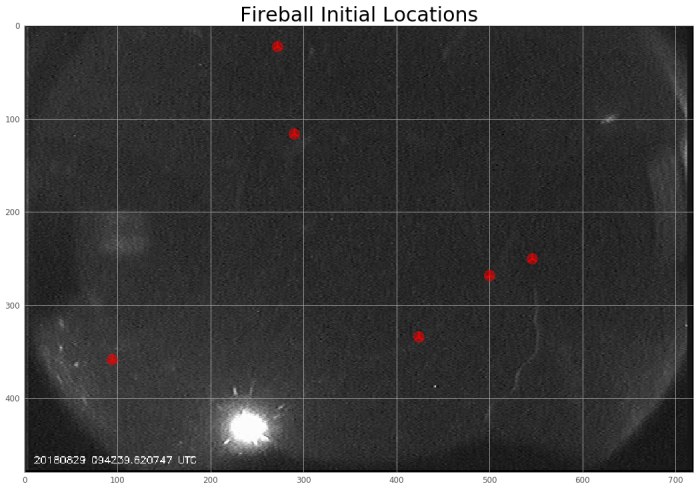

Figure 4.5: The initial pixel locations of all detected fireballs.

on 13 unique objects. Of these objects, the brightest had a Vmag, or apparent magnitude of 2. This star is Alpheratz.

5 Conclusion

Calculating average flux only depends on three variables. Although this calculation appears simple, estimating an average observational area can extremely difficult. Through establishing a versatile method for calculating observable sky area, we can now estimate the D6 AllSky Camera's average flux and compare it to other systems. As of this point, our data sample is too small to make any conclusive claims. There are still steps that need to be taken to truly assess the feasibility of using the D6 AllSky Camera in fireball research. This section will detail some of our self-assessed points of critique as well as shed light on some possible future research directions.

5.1 Results

After attaining the number of events, total observation time, and average observational area, we found that the D6 AllSky Camera had an average flux of 3.86×10^{-7} $\text{hr}^{-1}\text{km}^{-2}$. Table 5.1 displays this value alongside the values that contributed to our flux calculation. As a point of comparison, Dr. Jed Rembold measured an average flux rate of 1.09×10^{-7} $\text{hr}^{-1}\text{km}^{-2}$ when studying meteor impacts on the moon. The moon and earth are inherently two different objects with different gravitational effects. However they have similar locations with respect to our solar system, implying that their average flux rates should share some resemblance. The fact that the D6 AllSky Camera's fireball flux rate is of the same order of magnitude as research in the same field, we remain cautiously optimistic about the feasibility of our camera system.

5.2 Critique

While there are a multitude of positives to take away from this research, there are many areas of improvement as well. The main critique of our work stems from a

	Value	Units
Number of Events	6	events
Average Area	$56,012.03$	km^2
Total Time	291.87	hr
Flux	3.86×10^{-7}	$hr^{-1}km^{-2}$

Table 5.1: A display of our average flux rate alongside contributing variables.

lack of sufficient data. Flux estimates rely on a robust data sample, something that we were not able to attain in the academic year. In the Fall of 2018, we also experienced some camera difficulties that led to data that was incompatible with our Photometry GUI software.

5.2.1 Data Size

Throughout the history of fireball research, a sufficient data size has proven to be a vital characteristic of most notable findings. In 1996, the Canadian camera network published a detailed analysis of the 259 fireballs captured by their system [4]. Peter Brown, one of the most recognized figures in fireball research, released a paper in 2002 that detailed an analysis of 300 fireballs as captured by the department of energy and defense [2]. Surveys like these two have the luxury of calculating detailed flux estimates for fireballs with different energies or masses. By binning fireballs that share similar properties, these research groups can measure relationships between likelyhood of impact and fireball properties. The value of average flux is often ignored and replaced by the more detailed fireball property flux estimates. This makes comparing our system to existing systems significantly more difficult.

Our system has captured a small fraction of the events found in the aforementioned research papers. Our lack of data isn't necessarily due to a lack of camera capability, and likely has to do with the total time observed. Observing a total of 34 nights out of a possible 221 yields a ratio of observing a little less than 16% of nights. This low ratio is partially due to poor weather. However, there were also nights where the camera was not placed outside due to scheduling complications. Observing for more nights and capturing a larger number of fireball events will allow for more points of comparison to existing surveys. This will in turn allow us to gain a stronger understanding of how our system compares to current professional systems.

5.2.2 Camera Difficulties

In the summer before the 2018-2019 academic calendar, the D6 AllSky Camera began having difficulty focusing on the night sky. This inevitably led t images and videos containing lots of systematic noise. Figure 5.1 depicts the difference between an image with low and high noise. From these two images, it is clear that images and videos with high noise are more difficult to analyze. Coincidentally, the photometry program created by Luke Russell in 2017 and 2018 was created using test snapshots and videos taken without any noise issues. The subsequent problem with noise led to an incompatibility with the photometry software. Specifically, the part of the program that tracked the fireball location across frames was unable to do so when noisy pixels were found nearby the fireball.

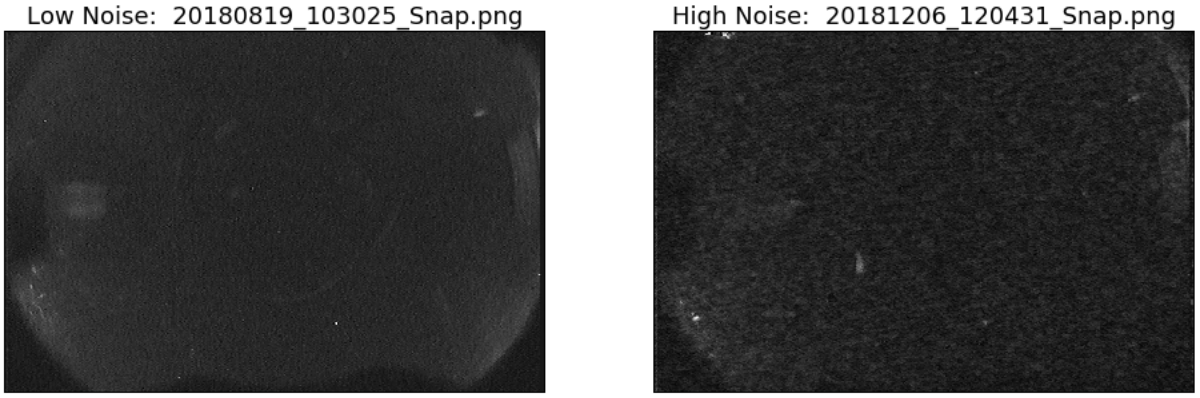

Figure 5.1: A D6 snapshot comparison of low and high noise.

Not only was the camera noise problematic for photometric analysis, but it also made star recognition more difficult. In a majority of the snapshots captured by the D6 AllSky Camera, we were unable to recognize any celestial objects. A lower-noise level would allow us to recognize more stars which would add to our star catalog, and increase the number of data points used to determine observable area. There is also a chance that we could detect dimmer stars with less-noisy data, leading to a stronger understanding of our camera's capabilities.

5.3 Outlook

Moving forward, the most important thing to focus on is data collection. Once the problem with unusually high volumes of systematic noise is dealt with, we will have most of the framework established to create a running fireball catalog. However, we will need to create a script that estimates a fireball's properties (energy, mass, size) given the photometry program's outputted light curve. This

project however should be fairly straightforward and will utilize the equations described in this papers background chapter.

While a singular camera can serve an important role in fireball research, systems with multiple cameras stationed in different locations have certain benefits. They allow for the triangulation of a given fireball which can then lead to stronger velocity and position estimates. With multiple systems, we could also estimate a fireball's orbital procession. Next year, we hope to construct another D6 AllSky camera that will lead to more precise data collection. The prospect of a secondary system is exciting and will hopefully help prove that the D6 AllSky camera is a desirable alternative in fireball research.

Bibliography

[1] Peter T Bobrowsky and Hans Rickman. "Comet/Asteroid Impacts and Human Society". In: (), p. 549.

[2] P Brown. "The flux of small near-Earth objects colliding with the Earth". In: 420 (Nov. 21, 2002), pp. 294–296.

[3] Peter Gural. "A review of video meteor detection and analysis software". In: (Feb. 23, 2005), p. 6.

[4] Ian Halliday, Arthur A. Griffin, and Alan T. Blackwell. "The Innisfree Meteorite Fall: A Photographic Analysis of Fragmentation, Dynamics and Luminosity". In: *Meteoritics* 16.2 (June 1, 1981), pp. 153–170. DOI: 10.1111/j.1945-5100.1981.tb00540.x.

[5] Stephen W Hughes et al. "The atmospheric extinction of light". en. In: *European Journal of Physics* 37.1 (Jan. 2016), p. 015601. DOI: 10.1088/0143-0807/37/1/015601.

[6] P. Jenniskens et al. "CAMS: Cameras for Allsky Meteor Surveillance to establish minor meteor showers". In: *Icarus* 216.1 (Nov. 1, 2011), pp. 40–61. DOI: 10.1016/j.icarus.2011.08.012.

[7] Jordi L. Pique. *PRESENTATION SPANISH PHOTOGRAPHIC METEOR NETWORK*.

[8] Kyle McSwain. "Using An All-Sky Camera to Observe Fireballs and Characterize Near-Earth Meteoroids". Physics Theses. Willamette University, May 11, 2016.

[9] Peter Jenniskens. *Cameras for Allsky Meteor Surveillance (CAMS)*. Nov. 2018.

[10] Joe Rao, Space com Skywatching Columnist {\textbar} March 9, and 2012 02:41pm ET. *Venus and Jupiter Align: 3 Odd Facts About 2-Planet Tango*. Space.com. URL: https://www.space.com/14852-venus-jupiter-alignment-facts.html (visited on 11/09/2018).

[11] Luke Russell. "Photometry of Celestial Fireballs Using a Portable All-Sky Camera". English. Physics Thesis. Willamette University, May 2018.

[12] Duncan Steel. “Meteoroid orbits”. In: *Space Science Reviews* 78.3 (Nov. 1, 1996), pp. 507–553. DOI: 10.1007/BF00171928.

[13] Josep M. Trigo-Rodríguez et al. “The 2006 Orionid outburst imaged by all-sky CCD cameras from Spain: meteoroid spatial fluxes and orbital elements”. In: *Monthly Notices of the Royal Astronomical Society* 380.1 (Sept. 1, 2007), pp. 126–132. DOI: 10.1111/j.1365-2966.2007.11966.x.

[14] *WAT-902H2 ULTIMATE*.